Shell-Structure Phase of Magnetically Confined Strongly Coupled Plasmas

S. L. Gilbert, J. J. Bollinger, and D. J. Wineland
Time and Frequency Division, National Bureau of Standards, Boulder, Colorado 80303
(Received 4 March 1988)

We report the observation of shell structure in $^9Be^+$ nonneutral plasmas (ion clouds) confined in a Penning trap. Clouds containing up to 15000 ions (density $\approx 10^8$ cm^{-3}) were laser cooled to temperatures of about 10 mK. Under these conditions, the ions are strongly coupled and exhibit liquidlike and solidlike behavior through the formation of concentric shells. The shells were observed by direct imaging of the laser-induced ion fluorescence for values of the Coulomb coupling constant Γ ranging from about 20 to 200. The shell structure is compared with theoretical predictions.

PACS numbers: 32.80.Pj, 52.25.Wz

The ability to cool collections of electrons or ions to temperatures where the Coulomb repulsion may produce a spatially ordered state has stimulated interest in several fields of physics. Detailed studies have been made in two-dimensional Coulomb systems[1] and in charged particles interacting through a shielded Coulomb potential.[2] In work more closely related to that described here, crystal-like structures of small numbers (<100) of macroscopic charged particles[3] and atomic ions[4] in Paul rf traps have been observed. The experiments on atomic ions appeared to be limited to small numbers because of the presence of rf heating,[5] which elevates the ion temperature in larger samples. Possibilities also exist for the observation of ordered structures of ions in storage rings.[6,7]

In Penning-type traps, where ions are confined by static electric and magnetic fields, rf heating does not take place and large collections of ions can be cooled to temperatures less than 10 mK. Several molecular-dynamics simulations on collections of a hundred to a few thousand ions confined in storage rings and traps have recently been completed.[7-10] Under conditions of strong coupling where the Coulomb potential energy between nearest neighbors is greater than the ion thermal energy, the ions are predicted to reside in concentric shells. Experimentally, strong coupling has been reported in systems of ions[11] and electrons[12] confined in Penning-type traps, but no evidence for spatial correlation was obtained. Here we report direct evidence for spatial correlation in magnetically confined ions. In clouds of laser-cooled $^9Be^+$ ions we observed structures containing from one shell (≈ 20 ions) to sixteen shells (≈ 15000 ions). The larger clouds may be approaching the infinite volume regime in which a bcc structure is predicted.[13]

The static thermodynamic properties of an ion cloud confined in a Penning trap are identical to those of a one-component plasma (OCP).[14] An OCP consists of a single species of charge embedded in a uniform-density background of opposite charge. For the system of ions in a Penning trap, the trapping fields play the role of the neutralizing background charge. An OCP is characterized by the Coulomb coupling constant,[13,14]

$$\Gamma \equiv q^2/a_s k_B T, \tag{1}$$

which is a measure of the nearest-neighbor Coulomb energy divided by the thermal energy of a particle. The quantities q and T are the ion charge and temperature. The Wigner-Seitz radius a_s is defined by $4\pi a_s^3 n_0/3 = 1$, where $-qn_0$ is the charge density of the neutralizing background. An infinite OCP is predicted[13] to exhibit liquidlike behavior (short-range order) for $\Gamma > 2$ and have a liquid-solid phase transition to a bcc lattice at $\Gamma = 178$.

For a finite plasma consisting of a hundred to a few thousand ions, the boundary conditions are predicted to have a significant effect on the plasma state. Simulations involving these numbers of ions have been done for the conditions of a spherical trap potential.[8-10] These simulations predict that the ion cloud will separate into concentric spherical shells. Instead of a sharp phase transition, the system is expected to evolve gradually from a liquid state characterized by short-range order and diffusion in all directions, to a state where there is diffusion within a shell but no diffusion between the shells (liquid within a shell, solidlike in the radial direction), and ultimately to an overall solidlike state.[10] These conclusions should apply to a nonspherical trap potential as well if the spherical shells are replaced with shells approximating spheriods. Preliminary independent investigations[15,16] of the nonspherical case support this conjecture.

We have investigated this interesting system using $^9Be^+$ ions trapped in the cylindrical Penning trap shown schematically in Fig. 1. A magnetic field $\mathbf{B} = B\hat{\mathbf{z}}$ ($B = 1.92$ T) produced by a superconducting magnet confined the ions in the direction perpendicular to the z axis. A static potential V_0 between the end and central cylinders confined the ions in the z direction to a region near the center of the trap. The dimensions of the trap electrodes were chosen so that the first anharmonic term of the trapping potential was zero. Over the region near the trap center, the potential can be expressed (in cylin-

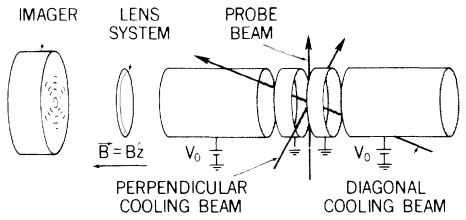

FIG. 1. Schematic drawing of the trap electrodes, laser beams, and imaging system (not to scale). The overall length of the trap is 10.2 cm. The trap consists of two end cylinders and two electrically connected central cylinders with 2.5-cm inner diameters. Ion clouds are typically less than 1 mm in both diameter and axial length. The diagonal cooling beam crosses the cloud at an angle of 51° with respect to the z axis.

drical coordinates) as $\Phi \cong AV_0(2z^2-r^2)$ where $A = 0.146\ \text{cm}^{-2}$. A background pressure of 10^{-8} Pa ($\approx 10^{-10}$ Torr) was maintained by a triode-sputter ion pump. The ions can be characterized by a thermal distribution where the "parallel" (to the z axis) temperature $T_\parallel$ is approximately equal to the "perpendicular" temperature $T_\perp$ (from the cyclotron motion). This thermal distribution is superimposed on a uniform rotation of the cloud[11,14] (frequency ω) which, at the low temperatures of this experiment, is due to the $\mathbf{E}\times\mathbf{B}$ drift, where $\mathbf{E}$ is the electric field due to the trap voltage and the space charge of the ions.

The ions were laser cooled and optically pumped into the $2s\ ^2S_{1/2}(M_I=\frac{3}{2}, M_j=\frac{1}{2})$ state by our driving the $2s\ ^2S_{1/2}(\frac{3}{2},\frac{1}{2}) \rightarrow 2p\ ^2P_{3/2}(\frac{3}{2},\frac{3}{2})$ transition slightly below the resonant frequency.[11] The 313-nm cooling radiation ($\approx 30\ \mu$W) could be directed perpendicular to the magnetic field and/or along a diagonal as indicated in Fig. 1. In addition to cooling the ions, the laser also applied an overall torque which could either compress or expand the cloud.[11] This allowed us to control the cloud size by choosing the radial positions (and thus the torques) of the perpendicular and diagonal beams.

About 0.04% of the 313-nm fluorescence from the decay of the $^2P_{3/2}$ state was focused by $f/10$ optics onto the photocathode of a resistive-anode photon-counting imaging tube. The imager was located along the z axis, about 1 m from the ions. The imaging optics was composed of a three-stage lens system with overall magnification of 27 and a resolution (FWHM) of about 5 μm (specifically, the image of a point source when referred to the position of the ions was approximately 5 μm in diameter). Counting rates ranged from 2 to 15 kHz. Positions of the photons arriving at the imager were displayed in real time on an oscilloscope while being integrated by a computer.

A second laser (power $\approx 1\ \mu$W, beam waist $\cong 30\ \mu$m) was used to map the shell structure of the cloud spatially. This probe laser was tuned to the same transition as the cooling laser and was directed through the

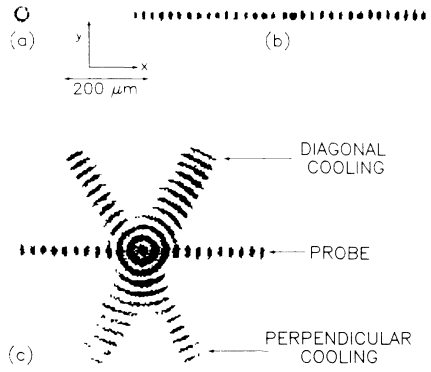

FIG. 2. Images of shell structures. (a) A single shell in a cloud containing approximately 20 ions. Trap voltage $V_0=14$ V and cloud aspect ratio a_r (axial length/diameter) $\cong 6.5$. This image was obtained from the ion fluorescence of the perpendicular and diagonal cooling beams. (b) Sixteen shells (probe-beam ion fluorescence only) in a cloud containing about 15000 ions with $v_0=100$ V and $a_r \cong 0.8$. (c) Eleven shells plus a center column in the same cloud as (b), with $V_0=28$ V and $a_r \cong 2.4$. This image shows the ion fluorescence from all three laser beams. Integration times were about 100 s for all images.

cloud perpendicularly to the magnetic field. With the probe laser on continuously, the cooling laser could be chopped at 1 kHz (50% duty cycle) and the image signal integrated only when the cooling laser was off. Different portions of the cloud could be imaged by the translation of the probe beam, in a calibrated fashion, either parallel or perpendicular to the z axis. Images were also obtained from the ion fluorescence of all three laser beams.

The probe beam was also used to measure the cloud rotation frequency ω and ion temperature.[11] For these measurements, the probe laser was tuned to the $2s\ ^2S_{1/2}(\frac{3}{2},\frac{1}{2}) \rightarrow 2p\ ^2P_{3/2}(\frac{3}{2},-\frac{1}{2})$ "depopulation" transition. Ions in the $2p\ ^2P_{3/2}(\frac{3}{2},-\frac{1}{2})$ state can decay to the $2s\ ^2S_{1/2}(\frac{3}{2},-\frac{1}{2})$ state, temporarily removing some of the ion population from the $2s\ ^2S_{1/2}(\frac{3}{2},\frac{1}{2})$ state. This results in a decrease in the cooling fluorescence as the probe laser is scanned through the depopulation transition. We determined ω by measuring the change in the Doppler shift of the depopulation signal as the probe beam was translated perpendicular to the z axis. The density n_0 could then be calculated[11,14] from $n_0 = m\omega(\Omega-\omega)/2\pi q^2$, where $\Omega = qB/mc$ is the cyclotron frequency. With use of n_0 and the cloud size obtained from probe-beam images, the total number of ions was calculated. The ion temperature was derived from the Doppler broadening contribution to the width of the depopulation signal.[11] The temperature $T_\perp$ was measured with the probe beam perpendicular to the magnetic field and $T_\parallel$ was measured by our sending the probe beam along the magnetic field direction (not shown in Fig. 1). In the latter case, crossed polarizers were used to reduce the intensity of the probe beam at the imager.

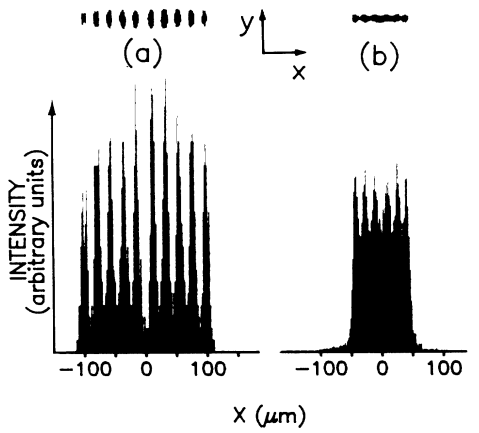

FIG. 3. Intensity plots along the imager x axis (parallel to the probe beam) through the center of the ion cloud with corresponding images (above). (a) $\Gamma = 180^{+90}_{-70}$ ($T = 6^{+4}_{-2}$ mK, $n_0 \cong 7\times10^7$ ions cm^{-3}). Cloud aspect ratio $a_r \cong 3.5$. (b) $\Gamma = 50^{+30}_{-20}$ ($T = 33^{+17}_{-13}$ mK, $n_0 = 2\times10^8$ ions cm^{-3}), $a_r \cong 5$. The clouds contained about 1000 ions in both cases.

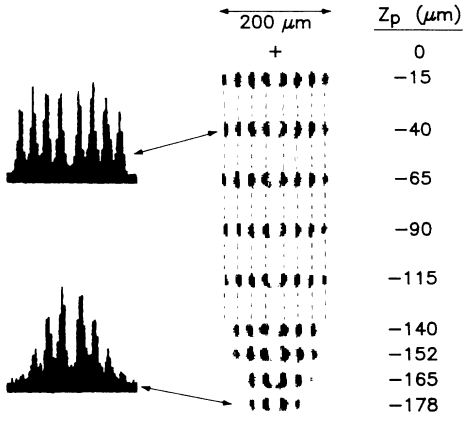

FIG. 4. Data showing evidence for concentric cylindrical shells. On the right is a series of images obtained with the probe beam for different z positions z_p of the probe beam (lower half of the cloud only). Intensity plots for $z_p = -40$ μm and $z_p = -178$ μm are shown on the left. The cloud aspect ratio a_r was about 1.9.

From the measured values of the temperature T and the density n_0, Γ was calculated with Eq. (1). In the case of $T_\perp \neq T_\parallel$, the larger temperature was used in the calculation of Γ.

We have observed shell structure in clouds containing as few as 20 ions (one shell) and in clouds containing up to about 15000 ions (sixteen shells). Images covering this range are shown in Fig. 2. We measured the coupling constant Γ for several clouds containing about 100 ions. Drift in the system parameters was checked by our verifying that the same images were obtained before and after the cloud rotation frequency and ion temperatures were measured. Figure 3 shows examples of shell structures at two different values of Γ. The first image is an example of high coupling ($\Gamma \approx 180$) showing very good shell definition in an intensity plot across the cloud. The second image is an example of lower coupling ($\Gamma \approx 50$) and was obtained with cooling only perpendicular to the magnetic field. Variations in peak intensities equidistant from the z axis are due to signal-to-noise limitations and imperfect alignment between the imager x axis and the probe beam.

We obtained three-dimensional information on the shell structure by taking probe images at different z positions. We found that there were two types of shell structure present under different circumstances. The first type showed shell curvature near the ends of the cloud, indicating that the shells may have been closed spheriods. Shell closure was difficult to verify because of a lack of sharp images near the ends of the cloud where the curvature was greatest. This may have been due to the averaging of the shells over the axial width of the probe beam. In the other type of shell structure, it was clear that the shells were concentric right circular cylinders with progressively longer cylinders near the center. An example of these data is shown in Fig. 4. Other evidence for cylindrical shells can be obtained from the fact that shells in the diagonal-beam images occur at the same cylindrical radii as those from the perpendicular beams. This can be seen in the three-beam images such as that shown in Fig. 2(c). Systematic causes of these two different shell configurations have not yet been identified.

One comparison which can be made between the theoretical calculations and our experimental results is the relationship between the number of shells and the number of ions, N_i, in a cloud. For a spherical cloud, approximately $(N_i/4)^{1/3}$ shells are predicted.[8] For the nearly spherical cloud of Fig. 2(b) ($N_i \cong 15000$) this formula predicts 15.5 shells and we measure 16. At present, it is difficult to make further quantitative comparisons between our data and the theoretical calculations. For example, there is substantial uncertainty in our measurement of Γ due to uncertainty in the temperature measurement. Our data do agree qualitatively with the simulations with the exception of the presence, in some cases, of an open-cylinder shell structure as opposed to the predicted closed spheroids. Schiffer has suggested[15] that shear (that is, different rotation frequencies) between the shells may account for this discrepancy. In our experiment, shear could be caused by differential laser torque or the presence of impurity ions.[17] For the data here, we have determined that the rotation frequency does not vary by more than 30% across the cloud. This is comparable to the limits discussed by Larson and co-workers.[17,18]

Future improvements will allow a more complete comparison of the data and the simulations, such as the rela-

tionship between shell definition and Γ for a variety of conditions. Also, we have observed that it is possible, using the probe depopulation transition, to tag ions in different parts of the cloud and see the presence (and lack) of ion diffusion. We plan to use this technique in a pulsed mode and obtain information on diffusion times within and between shells. Finally, with more laser power, even larger clouds (10^5 ions or more) can be cooled to these temperatures (10 mK). This may permit observation, by Bragg scattering,[11] of the predicted infinite volume structure.

We gratefully acknowledge the support of the U.S. Office of Naval Research and the Air Force Office of Scientific Research. We thank D. H. E. Dubin and J. P. Schiffer for useful discussions and C. Manney and W. Itano for help with image processing. We also thank G. Dunn, W. Itano, and C. Wieman for helpful suggestions on the manuscript.

[1]A. J. Dahm and W. F. Vinen, Physics Today **40**, No. 2, 43 (1987).

[2]D. J. Aastuen, N. A. Clark, and L. K. Cotter, Phys. Rev. Lett. **57**, 1733 (1986); J. M. di Meglio, D. A. Weitz, and P. M. Chaikin, Phys. Rev. Lett. **58**, 136 (1987); C. A. Murray and D. H. Van Winkle, Phys. Rev. Lett. **58**, 1200 (1987).

[3]R. F. Wuerker, H. Shelton, and R. V. Langmuir, J. Appl. Phys. **30**, 342 (1959).

[4]F. Diedrich, E. Peik, J. M. Chen, W. Quint, and H. Walther, Phys. Rev. Lett. **59**, 2931 (1987); D. J. Wineland, J. C. Bergquist, W. M. Itano, J. J. Bollinger, and C. H. Manney, Phys. Rev. Lett. **59**, 2935 (1987).

[5]D. A. Church and H. G. Dehmelt, J. Appl. Phys. **40**, 3421 (1969); H. G. Dehmelt, in *Advances in Laser Spectroscopy,* edited by F. T. Arecchi, F. Strumia, and H. Walther (Plenum, New York, 1983), p. 153.

[6]J. P. Schiffer and O. Poulsen, Europhys. Lett. **1**, 55 (1986).

[7]D. Habs, in "Frontiers of Particle Beams" (Springer-Verlag, Berlin, to be published).

[8]A. Rahman and J. P. Schiffer, Phys. Rev. Lett. **57**, 1133 (1986); J. P. Schiffer, to be published.

[9]H. Totsuji, in *Strongly Coupled Plasma Physics,* edited by F. J. Rogers and H. E. Dewitt (Plenum, New York, 1987), p. 19.

[10]D. H. E. Dubin and T. M. O'Neil, Phys. Rev. Lett. **60**, 511 (1988).

[11]J. J. Bollinger and D. J. Wineland, Phys. Rev. Lett. **53**, 348 (1984); L. R. Brewer, J. D. Prestage, J. J. Bollinger, and D. J. Wineland, in Ref. 9, p. 53.

[12]J. H. Malmberg, T. M. O'Neil, A. W. Hyatt, and C. F. Driscoll, in *Proceedings of the 1984 Sendai Symposium on Plasma Nonlinear Phenomena,* edited by N. Sato (Tohoku University, Sendai, Japan, 1984), p. 31.

[13]S. Ichimaru, H. Iyetomi, and S. Tanaka, Phys. Rep. **149**, 91 (1987), and references therein.

[14]J. H. Malmberg and T. M. O'Neil, Phys. Rev. Lett. **39**, 1333 (1977).

[15]J. P. Schiffer, private communication.

[16]D. H. E. Dubin, private communication.

[17]D. J. Larson, J. C. Bergquist, J. J. Bollinger, W. M. Itano, and D. J. Wineland, Phys. Rev. Lett. **57**, 70 (1986).

[18]L. R. Brewer, J. D. Prestage, J. J. Bollinger, W. M. Itano, D. J. Larson, and D. J. Wineland, Phys. Rev. A (to be published).

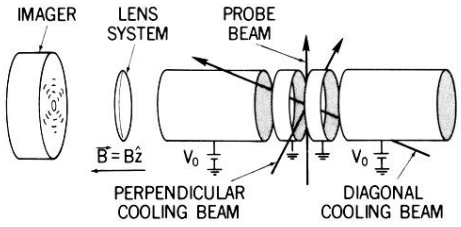

FIG. 1. Schematic drawing of the trap electrodes, laser beams, and imaging system (not to scale). The overall length of the trap is 10.2 cm. The trap consists of two end cylinders and two electrically connected central cylinders with 2.5-cm inner diameters. Ion clouds are typically less than 1 mm in both diameter and axial length. The diagonal cooling beam crosses the cloud at an angle of 51° with respect to the z axis.